Molecular Pharmacology Fast Forward. Published on March 28, 2007 as doi:10.1124/mol.107.034090
This article has not been copyedited and formatted. The final version may differ from this version.

MOL 34090

Proteasome Regulated ERBB2 and Estrogen Receptor Pathways in Breast Cancer

Corina Marx, Christina Yau, Surita Banwait, Yamei Zhou, Gary K. Scott,

Byron Hann, John W. Park, and Christopher C. Benz

(CM, CY, SB, YZ, GKS, CCB) Buck Institute for Age Research, Novato, CA, USA 94945.

(BH, JWP) Comprehensive Cancer Center, University of California, San Francisco, CA 94143.

Molecular Pharmacology Fast Forward. Published on March 28, 2007 as DOI: 10.1124/mol.107.034090
This article has not been copyedited and formatted. The final version may differ from this version.

MOL 34090

Running title: Proteasome regulated breast cancer pathways

To whom all correspondence should be addressed:

Christopher C. Benz, MD

Director, Cancer and Developmental Therapeutics Program

Buck Institute for Age Research,

8001 Redwood Blvd., Novato, CA 94945

tel.# 415-209-2092; fax# 415-209-2232; email: cbenz@buckinstitute.org

Text pages: 27

Tables: 1

Figures: 5

References: 27

Abstract: 249 words

Introduction: 640 words

Discussion: 1363 words

Abbreviations: HDAC, histone deacetylase; ER, estrogen receptor; UPS, ubiquitin-proteasome system.

Molecular Pharmacology Fast Forward. Published on March 28, 2007 as DOI: 10.1124/mol.107.034090
This article has not been copyedited and formatted. The final version may differ from this version.

Abstract

A major challenge to broadening oncology applications for inhibitors of the ubiquitin-proteasome system (UPS) is the identification of UPS-dependent cancer pathways predictive of tumors responsive to peptidomimetic inhibitors of its 20S core protease activity. To inform clinical studies evaluating UPS inhibitors as breast cancer therapeutics, seven phenotypically diverse human breast cancer cell line models were characterized for their cellular and molecular responses to the clinically approved 20S inhibitor, bortezomib (PS341, Velcade), focusing on those overexpressing estrogen receptor (ER) or ERBB2/HER2, as these oncogenic receptor pathways are constitutively activated in ~80% of all breast cancers. All models demonstrated dose-dependent bortezomib reduction in intracellular 20S activity correlating with cell growth inhibition; and bortezomib IC_{50} values (concentrations producing 50% growth inhibition) varied directly with pretreatment 20S activities ($r = 0.74$, $*p<0.05$), suggesting that basal 20S activity may serve as a clinical predictor of tumor responsiveness to UPS inhibition. Reduction in 20S activity (> 60%) was associated with early (24 h) intracellular relocalization of ER (nucleus to cytoplasm) and ERBB2 (plasma membrane to perinuclear lysosomes), buildup of ubiquitinated and Hsp70-associated receptor, degradation and loss of ER and ERBB2 function, and induction of cellular apoptosis. These models were also used to screen a pharmacologic panel of pathway-targeted anticancer agents (AG825, AZD6244/ARRY142886, LY294002, 17AAG, LAQ824) for those capable of sensitizing to bortezomib. In keeping with the observation that 20S reduction has little effect on MEK1/2 signaling in either ER-positive or ERBB2-positive models, only the MEK1/2 inhibitor AZD6244 consistently improved the antitumor activity of bortezomib.

Molecular Pharmacology Fast Forward. Published on March 28, 2007 as DOI: 10.1124/mol.107.034090
This article has not been copyedited and formatted. The final version may differ from this version.

Introduction

The 26S (2-MDa) multicatalytic ubiquitin-proteasome system (UPS) is responsible for the degradation of all short-lived and the majority of long-lived proteins in mammalian cells. The 20S axial pore complex possesses regulated protease activities, while the 19S multimeric cap components regulate the energy-dependent binding, unfolding, and entry of ubiquitin-tagged substrates into the 20S core, thereby directly controlling transcription, cell cycle progression and survival, as well as the elimination of misfolded and aggregated proteins formed in the cytosol, endoplasmic reticulum or nucleus (Voorhees and Orlowski, 2006). Despite this central role in all normal cell biology, the UPS has become a validated cancer therapeutic target following the clinical development of peptidomimetic small-molecule inhibitors of 20S core proteases and the 2003 FDA-approval of the dipeptide boronate, bortezomib (PS341, Velcade) for the treatment of refractory multiple myeloma (Kisselev et al., 2001; Voorhees and Orlowski, 2006). Not only are cancer cells apparently more dependent than normal cells on 26S-mediated degradation of growth and survival receptors, signaling intermediates and transcription factors, it has recently been shown in human breast cancer cell lines that growth factors also upregulate transcript and protein levels for the key ATPase subunit within the 19S complex that controls entry into the 20S core (Barnes et al., 2005).

While bortezomib selectively and reversibly inhibits the 20S chymotryptic site in UPS, newer and potentially more potent antitumor proteasome inhibitors capable of irreversibly inhibiting the 20S chymotryptic, tryptic and caspase sites have now entered clinical trials (Joazeiro et al., 2006). The antitumor activity of all proteasome inhibitors appears to be associated with induction of cell cycle arrest and apoptosis, commonly attributed to inhibition of NFκB (Wang et al., 1999; Feinman et al., 2004). However, different proteasome inhibitors can activate distinct pro-apoptotic pathways (Chauhan et al., 2005; Cusack et al., 2006), and a major challenge for broadening the clinical application of these novel agents is identifying which among the many pathways downstream of proteasome inhibition are most essential for and predictive of their anticancer activity (Joazeiro et al., 2006). Although bortezomib and newer proteasome inhibitors are being clinically evaluated partly because of their ability to sensitize or overcome resistance to standard chemotherapeutics, the choice of drugs for clinical

Molecular Pharmacology Fast Forward. Published on March 28, 2007 as DOI: 10.1124/mol.107.034090
This article has not been copyedited and formatted. The final version may differ from this version.

combination with these inhibitors remains largely empirical (Voorhees and Orlowski, 2006; Joazeiro et al., 2006). For the treatment of breast cancer in particular, bortezomib failed to show significant single-agent activity in initial clinical trials, leading to the recommendation that future clinical efforts target the UPS in specific subsets of breast cancer guided by more informative preclinical evidence (Cardoso et al., 2004; Dees and Orlowski 2006; Yang et al., 2006).

Recognizing the broad diversity of naturally occuring human breast cancers, we evaluated a clinically representative panel of seven phenotypically diverse human breast cancer cell line models and characterized their cellular and molecular responses to bortezomib, focusing on estrogen receptor (ER, alpha isoform) and ERBB2/HER2 receptor pathways since either of these pathways are constitutively activated in ~80% of all breast cancers. All cell lines in the panel demonstrated dose-dependent bortezomib reductions in intracellular 20S activity; and bortezomib IC_{50} (50% growth inhibitory concentration) values were found to correlate with pretreatment (basal) 20S proteasome activity. Downstream proteasome targets inhibited within 24 h of exposure to an IC_{50} bortezomib dose included ER and ERBB2 mechanisms in cell lines whose growth and survival are dependent on these receptor pathways. Surprisingly, bortezomib appeared relatively inefficient at inhibiting MEK1/2 generation of phospho-ERK1/2(44/42) in both ER-positive and ERBB2-positive breast cancer models. To guide future clinical studies, a pharmacologic panel of diverse pathway inhibitors was tested against the ER-positive and ERBB2-positive breast cancer models to identify targeted therapeutics able to enhance the anticancer activity of bortezomib. In keeping with the observation that 20S reduction produced little effect on MEK1/2 signaling in these models, a specific MEK1/2 inhibitor (AZD6244/ARRY142886) proved most capable of increasing the antitumor activity of bortezomib.

Molecular Pharmacology Fast Forward. Published on March 28, 2007 as DOI: 10.1124/mol.107.034090
This article has not been copyedited and formatted. The final version may differ from this version.

Materials and Methods

Cell Lines, Reagents, and Cell Viability Assay

The human breast cancer cell lines MCF7, SKBr3, BT474, MDA-453, T47D, and MDA-231 were originally obtained from American Type Culture Collection (ATCC, Rockville, MD) and were grown under ATCC-recommended conditions: 37°C, 5% CO2, and in Dulbecco's modified Eagle's medium, McCoys 5A, or RPMI-1640, supplemented with10% fetal bovine serum, 1% penicillin-streptomycin, and 10 ug/ml insulin. The MCF7/HER2 subline, overexpressing a constitutively hyperactive ERBB2 receptor kinase and possessing an altered endocrine phenotype, was developed as previously described (Benz et al., 1992). All media and supplements were purchased from Mediatech Inc. (Herndon, VA). Bortezomib was kindly provided by Millennium Pharmaceuticals (Cambridge, MA) and dissolved in DMSO in a 10uM stock stored in aliquots at -20°C. Sulforhodamine B reagent was purchased from Sigma-Aldrich (St. Louis, MO). The chemical inhibitor of ERBB2 kinase AG825 (4-Hydroxy-3-methoxy-5-(benzothiazolylthiomethyl)benzylidenecyanoacetamide), the PI3K inhibitor LY294002 (2-(4-Morpholinyl)-8-phenyl-4H-1-benzopyran-4-one hydrochloride) and the Hsp90 inhibitor 17-AAG (17-N-allylamino-17-demethoxy geldanamycin) were purchased from Calbiochem. AZD6244 (6-(4-Bromo-2-chloro-phenylamino)-7-fluoro-3-methyl-3H-benzoimidazole-5-carboxylic acid (2-hydroxy-ethoxy)-amide) was a kind gift of AstraZeneca (UK), and LAQ824 was a kind gift from Novartis Pharmaceuticals, Inc. (East Hanover, NJ). Treated and control cells were assayed for cell viability after plating in 12-well culture dishes at 20,000 cells per well and overnight attachment. Drug dissolved in media was added at the indicated concentrations and incubated at 37°C for 2 to 5 days; at the time of assay, 250ul of ice cold 50% trichloroacetic acid was added to each well and incubated at 4°C for 1 hour. Plates were washed 5 times with dH_2O before the addition of 500ul of sulforhodamine B (SRB, 0.4% in 1% acetic acid) and 30 minutes incubation at room temperature. Plates were rinsed 5 times in 1% acetic acid; the colored product was solubilized in unbuffered Tris base (pH 10.5) and quantified by absorbance at 564 nm. The optical density reading of 4 replicates for each treatment was normalized for the mean value of untreated cells and expressed as percent of control.

Molecular Pharmacology Fast Forward. Published on March 28, 2007 as DOI: 10.1124/mol.107.034090
This article has not been copyedited and formatted. The final version may differ from this version.

Human Breast Cancer Xenograft Model

Trastuzumab-resistant, ERBB2-positive B585 human breast cancer xenografts were grown in nude mice as described previously (Marx et al., 2006). Xenografts were serially passaged as subcutaneous tumors in the flanks of 4–6-week-old female nu/nu mice (Taconic Farms, Germantown, NY). B585 bearing mice were given intraperitoneal injections of vehicle or bortezomib (1 mg/kg) on days 15, 19, 22, 26, and 29; animal weights and three dimensional tumor measurements were determined at least twice weekly, and time-dependent mean (± SD) tumor volumes were calculated and plotted. Additional B585-bearing mice were given a single intraperitoneal injection of vehicle or 1 mg/kg PS-341 when B585 growth rates had achieved at least 300 mm3/ day; these mice were sacrificed 24 h after treatment in order to measure single-dose drug effects on resected and snap-frozen (-80°C) B585 tumors. Frozen samples were pulverized into a fine powder under liquid nitrogen for further assay. For protein analysis, tumor powders (0.02 g per sample) were homogenized by sonication (550 Sonic Dismembrator, Fisher Scientific, Pittsburgh, PA) twice for 15 s each in 100 ul of ice-cold extraction buffer (50 mM HEPES [pH 7.5], 100 mM NaCl, 2 mM Na3VO4, 1% Nonidet P-40, 0.01% SDS, and 1% deoxycholate) with/without a protease inhibitor cocktail (Mini Complete™, Roche Diagnostics, Mannheim, Germany).

20S Proteasome Activity Assay

Harvested cells or pulverized tumor tissues were lysed in buffer consisting of 50 mM HEPES [pH 7.5], 100 mM NaCl, 2 mM Na3VO4, 1% Nonidet P-40, 0.01% SDS, and 1% deoxycholate. Extracts were incubated on ice for 30 min and clarified by centrifugation for 15 min at 4°C. Protein concentration in the supernatant was determined using the Bradford assay (Bio-Rad, Hercules, CA). Approximately 50ug of total cell lysate was added to 0.5mM/L of LLVY-AMC (Chemicon) substrate and volumes were equalized in assay buffer (25mM HEPES, pH 7.5, 5mM EDTA, 0.5% NP-40, and 0.01 % SDS). Assay mixture was prepared in a 96-well fluorometer plate and incubated for 2 hours at 37°C. At the end of the incubation period, fluorescence was read using a 380/460 nm filter set in a fluorometer. A fluorescence standard curve with known dilutions of

Molecular Pharmacology Fast Forward. Published on March 28, 2007 as DOI: 10.1124/mol.107.034090
This article has not been copyedited and formatted. The final version may differ from this version.

substrate was generated in parallel with the assay samples and results were expressed in arbitrary fluorescence units per microgram of protein in the assay sample.

Immunoprecipitation and Immunoblot assays

For immunoblotting, harvested cells or pulverized tumor tissues were lysed in modified RIPA buffer (50 mM HEPES [pH 7.5], 100 mM NaCl, 2 mM Na3VO4, 1% Nonidet P-40, 0.01% SDS, and 1% deoxycholate) containing a protease inhibitor cocktail (Mini Complete™, Roche Diagnostics, Mannheim, Germany) and homogenized by sonication (550 Sonic Dismembrator, Fisher Scientific, Pittsburgh, PA) twice for 10 seconds each. Extracts were incubated on ice for 20 minutes and then clarified by centrifugation for 10 minutes at 4°C. Protein content of supernatants was determined by Bradford assay (Bio-Rad, Hercules, CA). 25-30 ug of lysate protein was heated to 95°C in 2x sample buffer (100 mM Tris [pH 6.8], 4% SDS, 20% glycerol, and 5% 2-mercaptoethanol) and electrophoresed in 4–12% Nu-Page Bis-Tris gradient gels (Invitrogen) with MOPS running buffer (Invitrogen). Separated proteins were transferred onto a polyvinylidene difluoride membrane (Millipore, Bedford, MA), blocked with 5% nonfat milk in phosphate-buffered saline containing 0.05% Tween 20, and probed sequentially with the antibodies listed below, stripping with Restore Western Blot Stripping Buffer (Pierce Biotechnology, Rockford, IL) in between each primary antibody probe. The following antibodies were used: mouse monoclonal anti-ERBB2/HER2 (Calbiochem), anti-phospho-HER2 (Tyr1248), rabbit polyclonal anti-phospho-AKT (Ser473) and anti-AKT, anti-phospho-ERK1/2(44/42) and anti-ERK1/2(44/42), anti-cyclin D1 (Cell Signaling Technology, Beverly, MA), mouse monoclonal anti-(p85)PARP (Promega Inc., Madison, WI), mouse monoclonal anti-beta actin (Abcam Inc., Cambridge, MA) and anti-ER alpha (Santa Cruz Biotechnology). Membranes were then incubated with horseradish peroxidase-linked secondary antibody (Bio-Rad), and signals were visualized using the enhanced chemiluminescence detection system (Amersham Pharmacia Biotech, Piscataway, NJ). For immunoprecipitation cells were treated as above and extracted in NP40 buffer containing 50 mM TrisHCl (pH 7.5), 150 mM NaCl, 1% Nonidet P-40, 10 mM NaF, 1 mM Sodium vanadate and a protease inhibitor cocktail (Mini Complete™, Roche Diagnostics, Mannheim, Germany) and homogenized by sonication. Protein

Molecular Pharmacology Fast Forward. Published on March 28, 2007 as DOI: 10.1124/mol.107.034090
This article has not been copyedited and formatted. The final version may differ from this version.

aliquots of 750 ug were precleared with Protein A sepharose beads, and then incubated with 5 ug of mouse monoclonal anti ErbB2 antibody (Calbiochem) for one hour at 4^{o}C under continuous agitation. Immune complexes were recovered by adding 50 ul of Protein A sepharose beads (Santa Cruz Biotechnology), washing x 3 in lysis buffer without NP-40 and resuspending in 50 ul of 2x Laemmli sample buffer prior to gel electrophoresis and immunoblotting as described above. For lysosomal protease inhibitor experiments SKBr3 cells were pre-treated with 100 uM Chloroquine for 1 hour before incubation with 10nM bortezomib for 48 hours. A second dose of Chloroquine was added 24 hours after the first dose. Cells lysates were prepared and analyzed by gel electrophoresis and immunoblotting as described.

Immunofluorescence Imaging

Cells were seeded in 8-chamber slides (Lab-Tek II) until subconfluent and treated with bortezomib as indicated. For SKBr3 and BT474 immunofluorescence experiments, cells were treated with bortezomib at 25 nM for 24 and 48 hours before fixing in PFA. For experiments with MCF7 cells and detection of the estrogen receptor, cells were serum starved for 24 or 48 hours before treatment. Cells were then treated with 25 nM bortezomib for 24 hours, and stimulated with 10 nM estradiol for 20 minutes before fixing. Cells were then washed with PBS and fixed with 4% PFA for 10 minutes at room temperature. After permeabilization in 0.5% Triton X for 10 minutes, cells were blocked in 5% serum of secondary antibody host diluted in TBS for 30 minutes at room temperature, and incubated in primary antibody diluted in 2.5% serum overnight. Primary antibodies used were mouse monoclonal anti-ERBB2/HER2 (Calbiochem) and anti-ER alpha (Santa Cruz Biotechnology). Secondary antibodies were donkey-anti mouse Alexa 488 and donkey anti-rabbit Alexa 555, diluted in 2.5% donkey serum and incubated for 30 minutes. Slides were mounted in Prolong Gold with DAPI and left overnight before fluorescent microscopic visualization and imaging.

NFκB DNA-binding Assays.

Quantitative p50 and p65 NFκB DNA-binding was determined using an ELISA-based Trans-AM^{TM} assay in accordance with the manufacturer's instructions (ActiveMotif;

Molecular Pharmacology Fast Forward. Published on March 28, 2007 as DOI: 10.1124/mol.107.034090
This article has not been copyedited and formatted. The final version may differ from this version.

Carlsbad, CA). In this commercial kit a duplexed NFκB oligonucleotide, containing the κB consensus binding sequence (5'-AGT TGA GGG GAC TTT CCC AGG C -3') is attached to the surface of 96-well plates. Activated NFκB in tumor extracts that is first bound to the attached oligonucleotide is specifically and quantitatively detected by subsequent incubation with p50 or p65 specific antibody followed by an enzyme (HRP)-linked secondary for colorimetric (OD_{450nm} absorbance) scoring.

Estrogen Responsive Transcriptional Reporter Assay.

Cultures were seeded one day before transfection with luciferase (luc) reporters to a density of 1-2 $x10^3$ cells per well in 96-well microtiter plates and using appropriate growth media. Cells were transiently transfected with 0.5 μg of (ERE)3-tk-luc reporter plasmid (Promega, Madison, MI) along with FuGene 6 transfection reagent (Roche, Indianapolis, IN). The Renilla luciferase vector pRL-tk-luc (Promega, Madison, MI) was co-transfected to normalize for transfection efficiency. Culture media was changed 20 h following transfection and cells were then treated with bortezomib (25 nM) for 24 h. Cells were subsequently washed with PBS, lysed for Dual-GloTM luciferase assay (Promega), and reporter activity measured by luminometer. Transfections were reported as fold-changes in luciferase activity over vehicle treated controls.

Molecular Pharmacology Fast Forward. Published on March 28, 2007 as DOI: 10.1124/mol.107.034090
This article has not been copyedited and formatted. The final version may differ from this version.

Results

Bortezomib Reduction in Breast Cancer Growth (IC_{50} values) and 20S Activity Correlates with Pretreatment (basal) 20S Proteasome Activity.

Exposure (72 h) of the human breast cancer cell line panel to increasing concentrations of bortezomib resulted in dose-dependent (Fig 1A) and time-dependent (Fig 1B) inhibition of cell growth, assessed by sulforhodamine B viability, and revealed different sensitivities to this proteasome inhibitor. ERBB2-positive SKBr3 cells showed the greatest sensitivity and lowest bortezomib IC_{50} (4 nM for 72 h exposure); in contrast, ERBB2-positive BT474 cells showed significantly reduced sensitivity and higher bortezomib IC_{50} (21 nM for 72 h exposure). Of note, constitutive overexpression of ERBB2 in ER-positive MCF7 with its endocrine altering consequences (Benz et al., 1992) produced modest bortezomib-sensitizing effects in MCF7/HER2 relative to parental MCF7 cells (MCF7/HER2 IC_{50} = 14 nM; MCF7 IC_{50} = 23 nM). The degree of inhibition of endogenous 20S proteasome activity within 24 h of bortezomib treatment generally correlated with bortezomib induced growth inhibition (Fig. 1C); exposure to IC_{50} bortezomib doses invariably reduced intracellular 20S proteasome activity to <40% of basal levels within 6 h. While there was no apparent correlation between bortezomib sensitivity and breast cancer clinical phenotype (ERBB2 and ER status), the pretreatment (basal) level of 20S proteasome activity in these cells correlated ($r = 0.74$, $^*p < 0.05$) with bortezomib IC_{50} value (Fig. 1D), indicating that breast cancer cells with lowest basal 20S proteasome activity are most sensitive to growth inhibition by bortezomib.

Proteasome Inhibition Causes Destabilization and Lysosomal Decay of ERBB2 with Reduction in phospho-AKT and Induction of Apoptosis.

Despite their differential sensitivity to bortezomib, the ERBB2-positive SKBr3 and BT474 cells showed similar intracellular responses to growth arresting and apoptosis inducing doses of bortezomib, suggesting that the ERBB2 dependent growth and survival mechanisms in these two cell lines are similarly dependent on the UPS. After 48 h treatment of the more sensitive SKBr3 cells with 5 nM bortezomib, apoptosis was induced as indicated by an increase in the caspase-3 mediated PARP1 cleavage product, p85 PARP; and this was associated with loss of phospho(Y1248)-ERBB2 and reduced

Molecular Pharmacology Fast Forward. Published on March 28, 2007 as DOI: 10.1124/mol.107.034090
This article has not been copyedited and formatted. The final version may differ from this version.

phospho-AKT (Fig. 2A) levels. For the less sensitive BT474 cells, this same response required a 25 nM dose of bortezomib. Surprisingly, phospho-ERK1/2 levels were not significantly altered in either cell line, indicating that an ERBB2 receptor-inhibiting and apoptosis-inducing dose of bortezomib does not impair activity of the mitogen activated protein kinase kinases, MEK1/2.

Since the Hsp90 chaperone protein is known to stabilize the active conformation of receptors like ERBB2 and their downstream signaling effectors like AKT (Calderwood et al, 2006, Xu et al, 2001), the early effect of bortezomib treatment on ERBB2 chaperone binding was evaluated by immunoprecipitation and immunoblotting. Within 24 h bortezomib treatment (10 nM) of either SKBr3 or BT474 cells, the association of Hsp90 with endogenous ERBB2 receptor was lost and replaced by another co-precipitating chaperone protein, Hsp70 (Fig. 2B). This altered chaperone binding occurred before significant loss in receptor content (Fig. 2A) but in conjunction with a buildup in ubiquitinated ERBB2 protein, detected in the same immunoprecipitates (data not shown).

At 24 h following bortezomib treatment of SKBr3 cells, immunofluorescent microscopic imaging was used to monitor the intracellular localization of the destabilized ERBB2 receptors. While vehicle treated cells showed only plasma membrane-localized ERBB2 receptor, chaperone-altering doses of bortezomib induced complete relocalization of ERBB2 within 24-48 h into a perinuclear cytoplasmic compartment (Fig. 2C) that co-localized with both immunoreactive lysosomal protein, LAMP1, and the endoplasmic reticulum marker, calreticulin (results not shown). A similar result was obtained with BT474 cells after 48 h of bortezomib treatment (results not shown). Co-treatment of SKBr3 cells with a non-toxic dose of the lysosomal processing inhibitor, chloroquine, prevented bortezomib induced ERBB2 decay in these cells. (Fig. 2D).

Phospho-AKT Reduction is associated with In vivo Inhibition of 20S Proteasome Activity and Reduced ERBB2-positive Breast Cancer Growth.

The trastuzumab-resistant, ERBB2-positive B585 human breast cancer xenograft model was used to determine the relative sensitivity of intratumor NFκB DNA-binding, phospho-ERK1/2 and phospho-AKT levels in response to bortezomib treatment sufficient

Molecular Pharmacology Fast Forward. Published on March 28, 2007 as DOI: 10.1124/mol.107.034090
This article has not been copyedited and formatted. The final version may differ from this version.

to reduce 20S proteasome activity and B585 growth in vivo. With maximally tolerated dosing of bortezomib (twice weekly 1 mg/kg intraperitoneal injections x4 into tumor bearing nude mice) nude mouse tumor volumes showed a modest growth inhibiting treatment effect, with mean tumor volumes determined after the second, third and fourth injections (days 22, 26 and 29) reduced no more than 30% relative to vehicle treated control mice (Fig. 3A). A parallel set of mice bearing palpable tumors growing at >300 mm3/ day were treated with a single intraperitoneal injection of either vehicle or bortezomib (1 mg/kg), and their tumors were resected 24 h later to assess intratumor 20S proteasome activity, NFκB (p50 and p65) DNA-binding, phospho-ERK1/2 and phospho-AKT levels. Tumors treated with a single injection of the growth inhibiting bortezomib dose showed a mean 40% reduction in intratumor 20S proteasome activity relative to the vehicle treated tumors (Fig. 3B). At this level of proteasome inhibition, tumor NFκB p50 and p65 DNA-binding activities were unaffected as were tumor phospho-ERK1/2 levels (Fig. 3C, 3D). In contrast, tumor phospho-AKT levels were reduced to 50% of control tumor levels (Fig. 3D).

Proteasome Inhibition Causes ER Relocalization and Decay with Loss of Transcriptional Function and Induction of Apoptosis.

Treatment of ER-positive MCF7 cells with growth inhibitory doses of bortezomib caused a marked dose-dependent reduction in ER content by 48 h (Fig. 4A); this was accompanied by loss of the proliferation marker cyclin D1, increase in the apoptosis marker p85 PARP, and a prominent increase in the pro-apoptotic and mitotic checkpoint protein, p53. However, significant changes in phospho-AKT or phospho-ERK1/2 levels were not detected (data not shown). To assess early effects of proteasome inhibition on ER function, MCF7 cells were transiently transfected with a luciferase reporter driven by an ERE-regulated promoter (ERE_3-TK-Luc); and as control for transfection efficiency and overall cell viability, a parallel set of MCF7 cells were transfected with a Renilla luciferase vector (TK-Luc). Following transient transfection (20 h), MCF7 treated with bortezomib (25 nM) for 24 hours showed a 40% specific reduction in ER transcriptional activity (ERE_3-TK-Luc activity), relative to vehicle treated cells or bortezomib treated MCF7 transfected with the TK-Luc vector (Fig. 4B). This early loss of ER transcriptional

Molecular Pharmacology Fast Forward. Published on March 28, 2007 as DOI: 10.1124/mol.107.034090
This article has not been copyedited and formatted. The final version may differ from this version.

activity preceding bortezomib induced loss of ER content suggested the possibility of a functional impairment in ER localization, as reported for other hormone receptors following proteasome inhibition (Shenoy et al. 2001, Yu et al. 2001, Lin et al. 2002). Immunofluorescence imaging for ER localization was performed on MCF7 cells treated with vehicle or bortezomib (25 nM, 24 h). While ER co-localized with DAPI nuclear staining in control cells, all bortezomib treated cells showed cytoplasmic localization of ER (Fig. 4C), indicating that bortezomib altered ER trafficking by inhibiting either cytoplasm-to-nucleus translocation or inducing nucleus-to-cytoplasm retrotranslocation of ER.

Pharmacologic Targeting of Pathways in Combination with Proteasome Inhibition.

To identify breast cancer targets that might complement proteasome inhibition, the panel of cell lines were treated for 48 h with IC_{50} bortezomib doses in combination with the following target inhibiting drugs and doses: histone deacetylases (LAQ824, 10nM), Hsp90 (17AAG, 50nM), ERBB2 kinase (AG825, 25μM), PI3K (LY294002, 10μM), or MEK1/2 (AZD6244, 100nM). The resulting growth inhibitory interactions were scored as antagonistic, additive, or supra-additive; however, no supra-additive bortezomib combinations were identified. Against ER-positive breast cancer cells (MCF7, BT474), only bortezomib combinations with LAQ824 or AZD6244 were additive. Against ERBB2-positive breast cancer lines (BT474, SKBr3), only bortezomib combinations with AG825 or AZD6244 were consistently additive. Against ER-negative cell lines (MDA231, SKBr3), only bortezomib in combination with AZD6244 was consistently additive. These drug interactions are summarized in Table 1; and the cell viability and growth effects of these representative drug-bortezomib interactions are demonstrated in Fig. 5. Of note, near additive interactions were observed in every cell line when the MEK1/2 inhibitor AZD6244 (100nM) was used in combination with an IC_{50} bortezomib dose.

Discussion

Codony-Servat et al. studied a panel of human breast cancer cell lines and measured a variety of cellular and molecular consequences following bortezomib

Molecular Pharmacology Fast Forward. Published on March 28, 2007 as DOI: 10.1124/mol.107.034090
This article has not been copyedited and formatted. The final version may differ from this version.

treatment, but were unable to identify any mechanism-based predictors of bortezomib responsiveness or pathway inhibitors capable of enhancing bortezomib sensitivity (Codony-Servat et al., 2006). To explore downstream markers of proteasome inhibition and pathways potentially targeted in combination with proteasome inhibitors, we studied a panel of seven human breast cancer cell line models representing clinically diverse phenotypes and expressing a wide range of endogenous 20S proteasome activities. All models demonstrated dose-dependent bortezomib reduction in intracellular 20S activity correlating with cell growth inhibition; and bortezomib IC_{50} values varied directly with pretreatment 20S activities ($r = 0.74$, $*p<0.05$), suggesting that basal 20S activity may serve as a clinical predictor of tumor responsiveness to UPS inhibition.

These breast cancer models also indicated that 6-24 h exposure to an IC_{50} bortezomib dose invariably reduced intracellular 20S activity by >60% from pretreatment levels. In contrast, the B585 xenograft study showed that maximally tolerated dosing of bortezomib produced only a 40% reduction in B585 20S proteasome activity. While this was associated with modest in vivo inhibition of B585 growth, the 40% reduction in B585 20S activity suggests that in vivo bortezomib bioavailability may be limiting for some solid tumors, insufficient to impact all the cancer pathways affected by an in vitro IC_{50} dose of bortezomib. However, these B585 xenograft studies confirmed that for ERBB2-positive breast cancers, reduction in phospho-AKT is a more sensitive indicator of 20S inhibition than either NFκB or MEK1/2 activity. With the clinical introduction of newer and more broadly acting proteasome inhibitors like NPI-0052 (Cusack et al., 2006; Joazeiro et al., 2006), it is reasonable to expect improved solid tumor bioavailability and greater inhibition of 20S proteasome activity, with resulting impairment of ERBB2 and ER breast cancer pathways at least comparable to those observed by in vitro treatment of our cell line models with IC_{50} bortezomib doses.

With >60% reduction in 20S proteasome activity, bortezomib inhibited cell growth by inducing cellular apoptosis (measured by increases in the caspase-3 mediated PARP1 cleavage product, p85), mediated in ER-positive and ERBB2-positive breast cancer models by different proteasome-dependent mechanisms. In the ER-positive MCF7 cell line model, down-regulation of ER content and transcriptional activity by bortezomib were associated with upregulation of the tumor suppressing protein, p53 (wildtype),

Molecular Pharmacology Fast Forward. Published on March 28, 2007 as DOI: 10.1124/mol.107.034090
This article has not been copyedited and formatted. The final version may differ from this version.

which undoubtedly contributed to the inhibition of cyclin D1 levels and cell cycle progression as well as induction of apoptosis detected by the caspase-3 mediated PARP1 cleavage product, p85. Within 24 h of MCF7 treatment, bortezomib induced a cytosolic buildup of ubiquitinated and Hsp70-associated undegraded ER (data not shown); these findings have been previously described and attributed to the critical function of the proteasome in maintaining nuclear receptor turnover and transcriptional activity (Lonard et al 2000, Reid et al 2003). Not previously reported is the observed bortezomib induced early relocalization of ER from nuclear to cytoplasmic compartments. Lin et al. (2002) found a similar response for androgen receptor (AR) following cellular treatment with the proteasome inhibitor MG132; in that study, proteasome inhibition for >24 h suppressed AR nuclear translocation by 50%, disrupted AR interactions with its co-regulators, and reduced total AR content of prostate cancer cells. Further studies are needed to understand the proteasome-dependent mechanisms regulating nuclear receptor trafficking.

Unlike the cell growth and survival mechanisms activated by overexpressed ER in MCF7 cells, the constitutive overexpression of ERBB2 receptor tyrosine kinase activity drives growth and survival of SKBR3 and BT474 breast cancer cells primarily by heterodimerization with and phosphorylation of the ERBB3 receptor, which serves to activate the downstream PI3K/AKT pathway. Within 48 h of a 20S reducing dose of bortezomib, surface membrane localized ERBB2 is lost in association with reduced phospho-AKT levels and the induction of cellular apoptosis in SKBr3 and BT474 cells, but without any detectable change in MEK1/2 activity as measured by phospho-ERK1/2 levels. The novel finding that 20S proteasome inhibition causes dissociation of the Hsp90 chaperone protein from ERBB2 receptor is similar to the reported ERBB2 effect induced by an Hsp90-inhibiting dose of benzoquinone ansamycins like geldanamycin or its clinical analog 17AAG (Xu et al, 2001). Treatment of ERBB2-positive cells with bortezomib, as with ansamycins, appears to shift ERBB2 chaperone association from one that is stabilizing (Hsp90) to one that is destabilizing (Hsp70). In ansamycin treated cells, dissociation of ERBB2 from Hsp90 is followed by proteasomal degradation of ERBB2; however, in cells treated with the proteasome inhibitor bortezomib, the loss of ERBB2 content must occur by a different mechanism. One contributing possibility is the recently

described repression of ERBB2 transcript levels caused by various proteasome inhibitors (Marx et al, 2006). A more likely explanation for the rapid loss of total ERBB2 content is that following proteasome inhibition the destabilized and ubiquitin-tagged ERBB2 is sequestered within perinuclear aggresomes where it is degraded by lysosomal proteases, consistent with the observed prevention of ERBB2 degradation by the lysosome inhibitor chloroquine. Microtubule-mediated transport and accumulation of polyubiquitinated proteins into aggresomes has recently been reported (Nawrocki et al., 2006 Johnston et al., 1998). However, further study of proteasome-dependent ERBB2 trafficking mechanisms is needed, since the observed perinuclear sequestration of ERBB2 could also have resulted from bortezomib induced disruption of normal ERBB2 endocytotic mechanisms (Austin et al., 2004).

Approximately 80% of human breast cancers overexpress ER and/or ERBB2 receptors. Despite available therapeutics that specifically target these overexpressed receptors, clinical resistance to these target-specific agents is common. Therefore, there is both clinical need and interest in applying proteasome inhibitors to improve the treatment of breast cancer (Cardoso et al., 2004; Dees and Orlowski 2006). However, because of the diversity of breast cancer phenotypes it is also appreciated that rational combination of proteasome inhibitors with other targeted therapeutics must be guided by informative preclinical studies (Yang et al., 2006). Based on the above observations that 20S proteasome inhibition can be cytotoxic to ER and ERBB2 overexpressing breast cancer cells by different mechanisms, our cell line models were used to screen a pharmacologic panel of diverse pathway inhibitors to identify targeted agents capable of sensitizing to bortezomib. The five targeted agents shown in Table 1 (AG825, AZD6244, LY294002, 17AAG, LAQ824) were tested at doses previously shown to inhibit their pathways, although when used as single agents these inhibitors produced quite variable cell line-dependent growth inhibition. The Hsp90 inhibitor, 17AAG, proved antagonistic in combination with bortezomib against all models tested; this finding is in contrast to the ansamycin result reported by Mimnaugh et al. (2004), although it is consistent with the fact that Hsp90 inhibitors induce proteasomal decay of Hsp90 client proteins (e.g. ER, ERBB2, AKT) which is not possible in the presence of effective 20S inhibition. The ERRB2 kinase inhibitor, AG825, and the PI3K inhibitor, LY294002, enhanced

Molecular Pharmacology Fast Forward. Published on March 28, 2007 as DOI: 10.1124/mol.107.034090
This article has not been copyedited and formatted. The final version may differ from this version.

bortezomib cytotoxicity but only in ERBB2-positive cells in which these target kinases are constitutively activated. The histone deacetylase (HDAC) inhibitor, LAQ824, was antagonistic to bortezomib only in the same ERBB2-positive breast cancer cell lines previously shown to be most sensitive to this and other HDAC inhibitors (Scott et al., 2002), suggesting that HDAC and proteasome mechanisms have overlapping and non-complementary growth regulating roles in ERBB2-positive but not ERBB2-negative malignant cell lines. This possibility deserves further study given the report that the shuttling of misfolded proteins into the aggressome, a potential consequence of proteasome inhibition, is HDAC dependent (Kawaguchi et al., 2003). Unlike the other targeted agents evaluated, only the MEK1/2 inhibitor AZD6244 proved capable of additively enhancing the growth inhibiting effect of bortezomib in all breast cancer models studied. Since bortezomib was relatively inefficient at inhibiting MEK1/2 in both ER-positive and ERBB2-positive breast cancer cells, and a MEK1/2 inhibiting dose of AZD6244 (100 nM), by itself, failed to significantly inhibit the growth of three of the breast cancer cell lines (SKBr3, BT474, MCF7), the observed additive interaction between AZD6244 and bortezomib suggests that each agent is acting on independent but complementary growth regulating mechanisms. Thus, when compared to the other targeted agents evaluated in these models, AZD6244 would appear to be the most promising agent for further preclinical evaluation in combination with a 20S inhibiting dose of bortezomib or newer generation proteasome inhibitor.

Molecular Pharmacology Fast Forward. Published on March 28, 2007 as DOI: 10.1124/mol.107.034090
This article has not been copyedited and formatted. The final version may differ from this version.

Acknowledgements

We thank Donghui Wang at UCSF for her technical assistance with the xenograft studies. Bortezomib was kindly provided by Millennium Pharmaceuticals (Cambridge, MA); AZD6244 was provided by AstraZeneca (UK); and LAQ824 was provided by Novartis Pharmaceuticals, Inc. (East Hanover, NJ).

References

Austin CD, De Maziere AM, Pisacane PI, van Dijk SM, Eigenbrot C, Sliwkowski MX, Klumperman J and Scheller RH (2004) Endocytosis and sorting of ErbB2 and the site of action of cancer therapeutics trastuzumab and geldanamycin. Mol Biol Cell **15**:5268-82.

Barnes CJ, Li F, Talukder AH and Kumar R (2005) Growth factor regulation of a 26S proteasomal subunit in breast cancer. Clin Cancer Res **11:**2868-74.

Benz CC, Scott GK, Sarup JC, Johnson RM, Tripathy D, Coronado E, Shepard HM and Osborne CK (1992) Estrogen-dependent, tamoxifen-resistant tumorigenic growth of MCF-7 cells transfected with HER2/neu. Breast Cancer Res Treat **24**:85-95.

Calderwood SK, Khaleque MA, Sawyer DB and Ciocca DR (2006) Heat shock proteins in cancer: chaperones of tumorigenesis. Trends Biochem Sci. **31**:164-72.

Cardoso F, Ross JS, Picart MJ, Sotiriou C and Durbecq V (2004) Targeting the ubiquitin-proteasome pathway in breast cancer. Clin Breast Cancer **5**:148-57.

Chauhan D, Catley L, Li G, Podar K, Hideshima T, Velankar M, Mitsiades C, Mitsiades N, Yasui H, Letai A, Ovaa H, Berkers C, Nicholson B, Chao TH, Neuteboom ST, Richardson P, Palladino MA and Anderson KC (2005) A novel orally active proteasome inhibitor induces apoptosis in multiple myeloma cells with mechanisms distinct from Bortezomib. Cancer Cell **8**:407-19.

Codony-Servat J, Tapia MA, Bosch M, Oliva C, Domingo-Domenech J, Mellado B, Rolfe M, Ross JS, Gascon P, Rovira A and Albanell J (2006) Differential cellular and molecular effects of bortezomib, a proteasome inhibitor, in human breast cancer cells. Mol Cancer Ther **5**:665-75 .

Cusack JC Jr, Liu R, Xia L, Chao TH, Pien C, Niu W, Palombella VJ, Neuteboom ST and Palladino MA (2006) NPI-0052 enhances tumoricidal response to conventional cancer therapy in a colon cancer model. Clin Cancer Res **12(22):**6758-64.

Dees EC and Orlowski RZ (2006) Targeting the ubiquitin-proteasome pathway in breast cancer therapy. Future Oncol **2**:121-35.

Feinman R, Siegel DS and Berenson J (2004) Regulation of NF-kB in multiple myeloma: therapeutic implications. Clin Adv Hematol Oncol **2**:162-6.

Joazeiro CA, Anderson KC and Hunter T (2006) Proteasome inhibitor drugs on the rise. Cancer Res **66**:7840-2.

Johnston JA, Ward CL and Kopito RR (1998) Aggresomes: a cellular response to misfolded proteins. J Cell Biol **143**:1883-98.

Kawaguchi Y, Kovacs JJ, McLaurin A, Vance JM, Ito A and Yao TP (2003) The deacetylase HDAC6 regulates aggresome formation and cell viability in response to misfolded protein stress. Cell **115**:727-38.

Kisselev AF and Goldberg AL (2001) Proteasome inhibitors: from research tools to drug candidates. Chem Biol **8**:739-58.

Lin HK, Altuwaijri S, Lin WJ, Kan PY, Collins LL and Chang C (2002) Proteasome activity is required for androgen receptor transcriptional activity via regulation of androgen receptor nuclear translocation and interaction with coregulators in prostate cancer cells. J Biol Chem **277**:36570-6.

Lonard DM, Nawaz Z, Smith CL and O'Malley BW (2000) The 26S proteasome is required for estrogen receptor-alpha and coactivator turnover and for efficient estrogen receptor-alpha transactivation. Mol Cell **5(6):**939-48.

Marx C, Berger C, Xu F, Amend C, Scott GK, Hann B, Park JW, Benz CC (2006) Validated high-throughput screening of drug-like small molecules for inhibitors of ErbB2 transcription. Assay Drug Dev Technol **4**:273-84.

Mimnaugh EG, Xu W, Vos M, Yuan X, Isaacs JS, Bisht KS, Gius D and Neckers L (2004) Simultaneous inhibition of hsp 90 and the proteasome promotes protein ubiquitination, causes endoplasmic reticulum-derived cytosolic vacuolization, and enhances antitumor activity. Mol Cancer Ther **3**:551-66.

Nawrocki ST, Carew JS, Pino MS, Highshaw RA, Andtbacka RH, Dunner K Jr, Pal A, Bornmann WG, Chiao PJ, Huang P, Xiong H, Abbruzzese JL and McConkey DJ (2006) Aggresome disruption: a novel strategy to enhance bortezomib-induced apoptosis in pancreatic cancer cells. Cancer Res **66**:3773-81.

Reid G, Hubner MR, Metivier R, Brand H, Denger S, Manu D, Beaudouin J, Ellenberg J and Gannon F. (2003) Cyclic, proteasome-mediated turnover of unliganded and liganded ERalpha on responsive promoters is an integral feature of estrogen signaling. Mol Cell **11**:695-707.

Scott GK, Marden C, Xu F, Kirk L and Benz CC (2002) Transcriptional repression of ErbB2 by histone deacetylase inhibitors detected by a genomically integrated ErbB2 promoter-reporting cell screen. Mol Cancer Ther **1**:385-92.

Shenoy SK, McDonald PH, Kohout TA and Lefkowitz RJ (2001) Regulation of receptor fate by ubiquitination of activated beta 2-adrenergic receptor and beta-arrestin. Science **294(5545):**1307-13.

Voorhees PM and Orlowski RZ (2006) The proteasome and proteasome inhibitors in cancer therapy. Annu Rev Pharmacol Toxicol **46**:189-213.

Wang CY, Cusack JC Jr, Liu R and Baldwin AS Jr (1999) Control of inducible chemoresistance: enhanced anti-tumor therapy through increased apoptosis by inhibition of NF-kappaB. Nat Med **5**:412-7.

Xu W, Mimnaugh E, Rosser MF, Nicchitta C, Marcu M, Yarden Y and Neckers L (2001) Sensitivity of mature Erbb2 to geldanamycin is conferred by its kinase domain and is mediated by the chaperone protein Hsp90. J Biol Chem **276**:3702-8.

Yang CH, Gonzalez-Angulo AM, Reuben JM, Booser DJ, Pusztai L, Krishnamurthy S, Esseltine D, Stec J, Broglio KR, Islam R, Hortobagyi GN and Cristofanilli M (2006) Bortezomib (VELCADE) in metastatic breast cancer: pharmacodynamics, biological effects, and prediction of clinical benefits. Ann Oncol **17**:813-7.

Yu A and Malek TR (2001) The proteasome regulates receptor-mediated endocytosis of interleukin-2. J Biol Chem **276**:381-5.

Molecular Pharmacology Fast Forward. Published on March 28, 2007 as DOI: 10.1124/mol.107.034090
This article has not been copyedited and formatted. The final version may differ from this version.

Footnotes

This research was supported in part by NIH sponsored grants R01-CA36773 and R01-CA701468 (Buck Institute) and P50-CA58207 (UCSF Breast SPORE), research sponsorship from Millennium Pharmaceuticals Inc. to the UCSF Comprehensive Cancer Center, and Hazel P. Munroe memorial funding to the Buck Institute.

Molecular Pharmacology Fast Forward. Published on March 28, 2007 as DOI: 10.1124/mol.107.034090
This article has not been copyedited and formatted. The final version may differ from this version.

Figure Legends

Figure 1. Bortezomib inhibition of breast cancer cell growth and 20S proteasome activity, and correlation with pretreatment 20S activity. A. Dose-dependent growth inhibition of seven different human breast cancer cell line models by the indicated bortezomib (PS341) concentrations, assessed by sulforhodamine B (SRB) cell viability at 72 h. Data points represent mean (± SD) SRB values relative to vehicle treated controls; growth inhibitory effects on each cell line are summarized as bortezomib IC_{50} values (concentrations causing 50% growth inhibition). **B.** Time-dependent growth inhibition of the seven different breast cancer cell lines exposed to a single concentration of bortezomib (5 nM). **C.** 20S proteasome levels measured from extracts of each breast cancer cell line 24 h following vehicle (0 nM) or PS341 (5 or 25 nM) treatment using the fluorogenic LLVY-AMC substrate. Results are expressed as mean (± SD) 388/460 nm fluorescence activity of 20S generated substrate per microgram cell line extract. **D.** Correlation between baseline (untreated) cell line 20S proteasome activity and bortezomib IC_{50} values, with correlation coefficient and *p value calculated by Pearson's correlation test.

Figure 2. Early in vitro effects of proteasome inhibition on ERBB2 receptor chaperone binding, intracellular localization, and cell survival signaling. A. ERBB2 overexpressing SKBr3 and BT474 breast cancer cells were treated with the indicated growth suppressing concentrations of bortezomib (PS341) prior to extraction and immunoblotting to monitor levels of total ERBB2, AKT, ERK1/2 and actin, as well as phospho(p)-ERBB2, phospho(p)-AKT and the caspase-cleaved apoptotic product, p85 PARP. **B.** Cell lysates of vehicle or bortezomib (10 nM x 24 h) treated SKBr3 and BT474 cells were subjected to ERBB2 immunoprecipitation (IP), and the co-precipitated proteins were then Western imunoblotted (WB) to measure chaperone binding to ERBB2 by either Hsp90 or Hsp70. **C**. ERBB2 receptor distribution relative to DAPI nuclear staining visualized by co-immunofluorescence at 24 h after vehicle (control) or bortezomib (10 nM) treatment of SKBr3 cells; merged images show predominantly cell surface ERBB2 localization in control cells and perinuclear cytoplasmic ERBB2

Molecular Pharmacology Fast Forward. Published on March 28, 2007 as DOI: 10.1124/mol.107.034090
This article has not been copyedited and formatted. The final version may differ from this version.

localization in treated cells. **D.** Immunoblots of extracts from control and bortezomib (10 nM x 24 h) treated SKBr3 cells with/without co-treatment using a non-toxic dose of the lysosomal processing inhibitor, chloroquine (100 μM).

Figure 3. In vivo effects of maximally tolerated bortezomib dosing on B585 breast cancer growth, 20S proteasome and NFκB activities, phospho-ERK1/2 and phospho-AKT levels. A. Mean (± SD) B585 tumor volumes (10 tumor bearing mice per treatment arm) on the indicated days (22, 26, 29) and following the second, third and fourth injections (intraperitoneal) of either vehicle (C) or a maximally tolerated twice weekly dosing of bortezomib (PS341; 1 mg/kg). **B-D.** Additional B585-bearing mice (three per treatment group) were given a single injection of either vehicle (C) or bortezomib (PS341, 1 mg/kg) when tumor growth rates achieved >300 mm^3/day; tumors were excised 24 h later to assess drug effects on 20S proteasome and NFκB (p50, p65 subunits) DNA-binding activities, phospho-ERK1/2 and phospho-AKT levels, as indicated and described in methods. Bar graphs represent mean (± SD) activities or normalized immunoblot band intensities quantitated by densitometric scanning.

Figure 4. Early in vitro effects of proteasome inhibition on ER receptor content, intracellular localization and transcriptional activity, cell proliferation and survival signals. A. ER overexpressing MCF7 breast cancer cells were treated with the indicated growth suppressing concentrations of bortezomib (PS341) prior to extraction and immunoblotting to measure levels of total ER (alpha isoform), cyclin D1, p53, actin, and the caspase-cleaved apoptotic product, p85 PARP. **B.** Following transient transfection of MCF7 cells with either ERE_3-TK-Luc (luciferase) or TK-Luc (Renilla luciferase) reporters, cell cultures were treated with vehicle or bortezomib (25 nM x 24 h), and then lysates were analyzed and mean (± SD) fold-changes in luciferase activity over vehicle treated control reporter activity recorded. **C.** Intracellular ER (green) was localized by immunofluorescence microscopy 24 h after vehicle or bortezomib (25 nM) treatment of MCF7 cells (left panels), as described in methods. DAPI (blue) was used to counterstain MCF7 cell nuclei in the same field (middle panels). Merging of green stained ER and

Molecular Pharmacology Fast Forward. Published on March 28, 2007 as DOI: 10.1124/mol.107.034090
This article has not been copyedited and formatted. The final version may differ from this version.

blue stained nuclear images demonstrates overlapping nuclear origin of ER signals in control MCF7, but distinct perinuclear origin of ER signals in treated cells (right panels).

Figure 5. Representative growth inhibitory interactions between bortezomib and other pathway-targeted antitumor agents. For each of the four breast cancer cell lines indicated, an IC_{50} bortezomib dose was combined over 48 h with a target-inhibiting dose of the ERBB2 kinase inhibitor AG825 (**A;** 25 nM), the MEK1/2 inhibitor AZD6244 (**B**; 100 nM), the PI3K inhibitor LY294002 (**C**; 10 μM), the Hsp90 inhibitor 17AAG (**D**; 50 nM), or the HDAC inhibitor LAQ824 (**E**; 10 nM). Growth inhibition was assessed using the sulforhodamine B cell viability assay as described in methods; and results expressed as mean (± SD) percent cell viability relative to vehicle treated controls.

Molecular Pharmacology Fast Forward. Published on March 28, 2007 as DOI: 10.1124/mol.107.034090
This article has not been copyedited and formatted. The final version may differ from this version.

Table 1. Summary of antagonistic (-) or additive (+) cell growth effects of targeted agents tested in combination with bortezomib (IC_{50} dose) against the indicated breast cancer cell line models.

Target Inhibitor (dose)	**MDA-231** (ERBB2-/ER-)	**SKBr3** (ERBB2+/ER-)	**BT474** (ERBB2+/ER+)	**MCF7** (ERBB2-/ER+)
ErbB2 kinase AG825 (25uM)	-	+	+	-
MEK1/2 AZD6244 (100nM)	+	+	+	+
PI3K LY294002 (10uM)	-	+	+	-
Hsp90 17AAG (50nM)	-	-	-	-
HDACs LAQ824 (10nM)	+	-	-	+

Figure 1

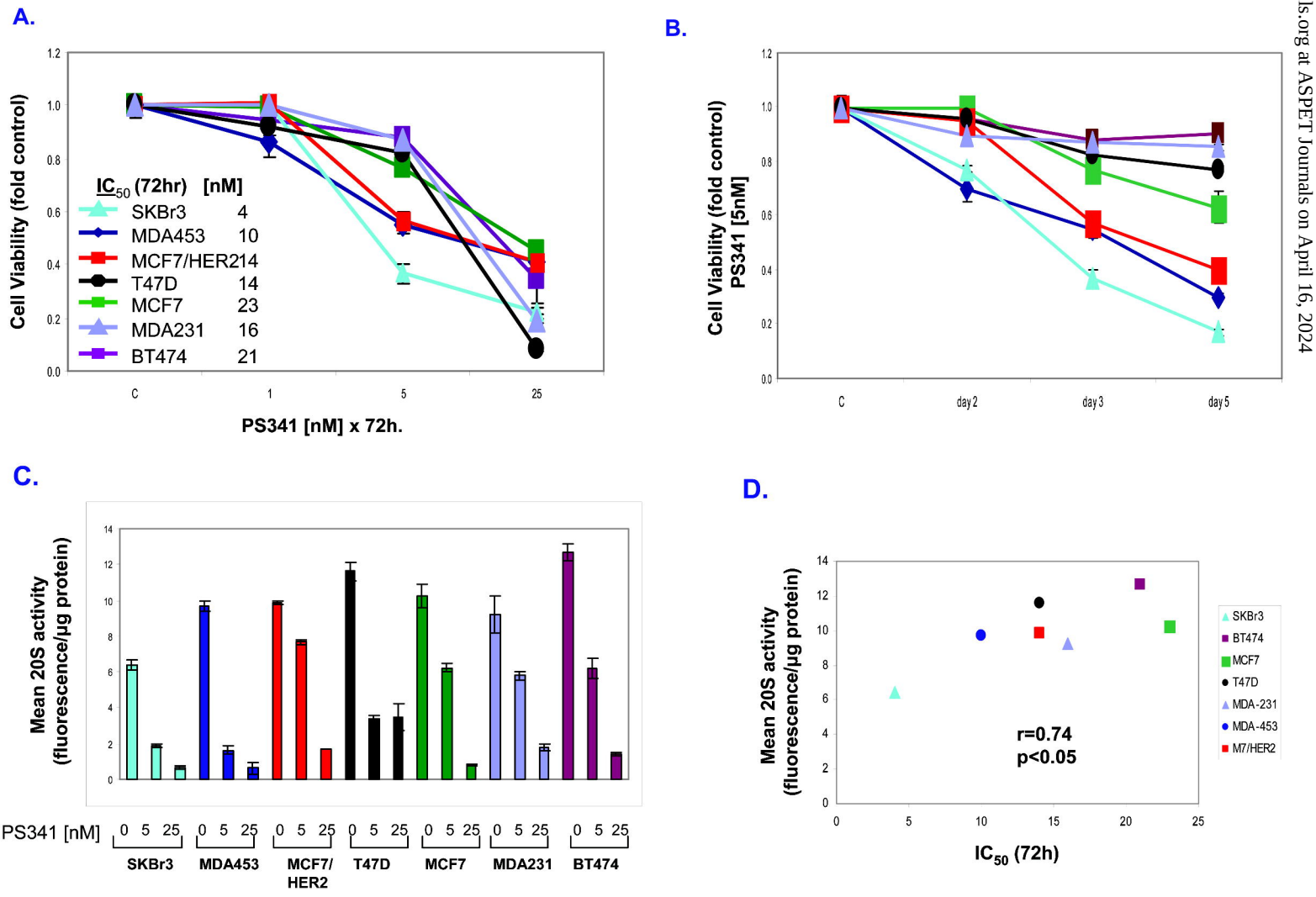

Figure 2

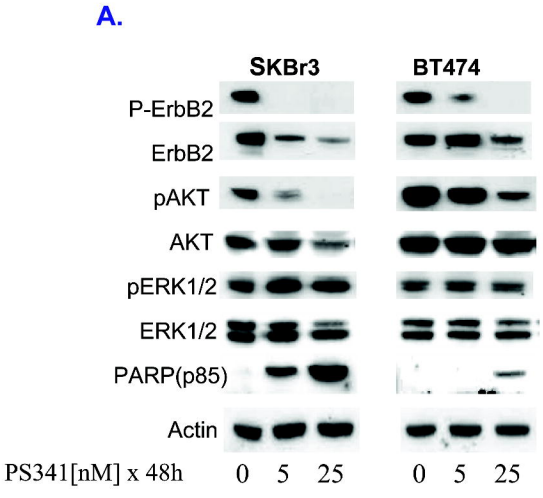

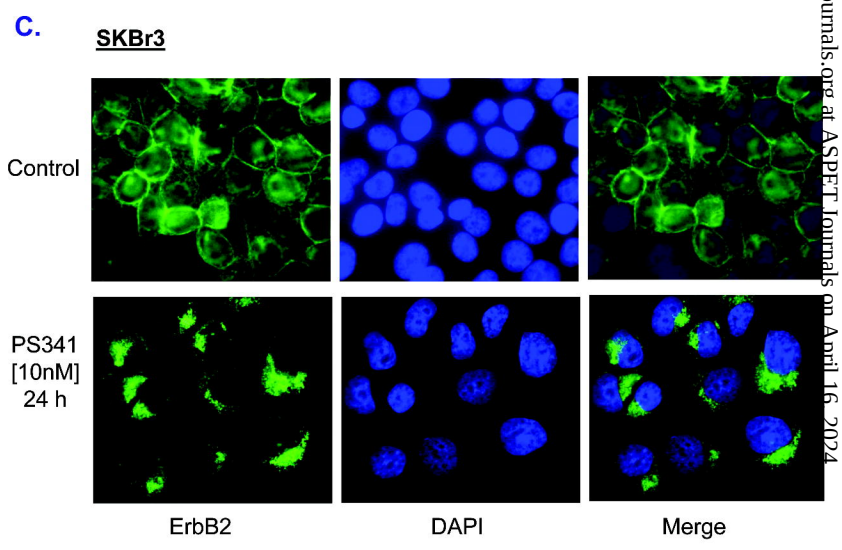

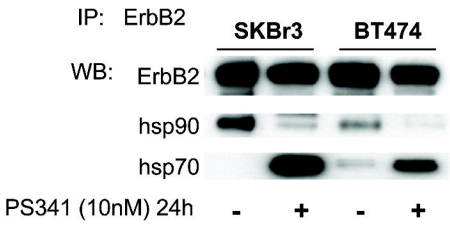

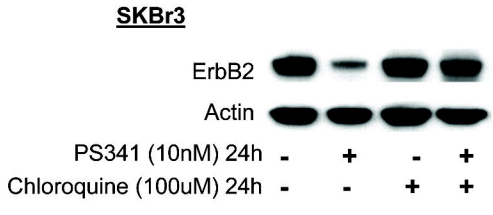

Figure 3

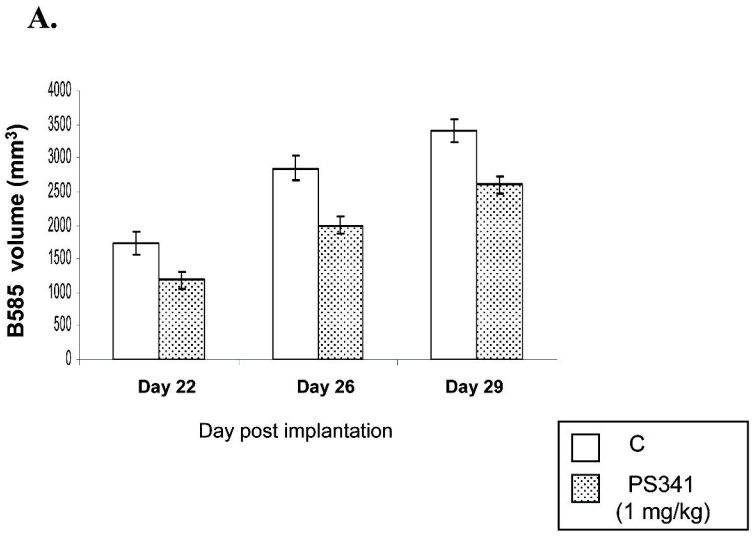

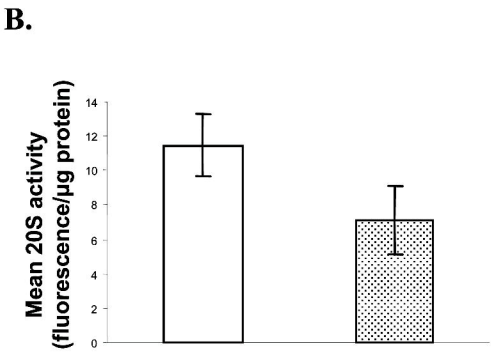

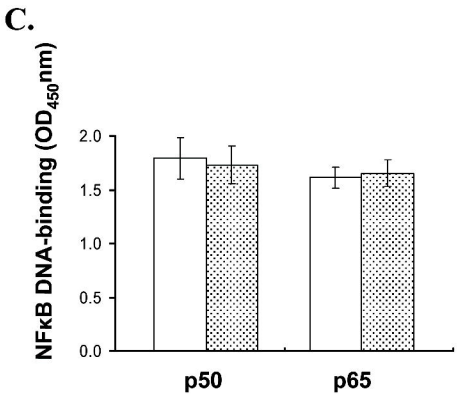

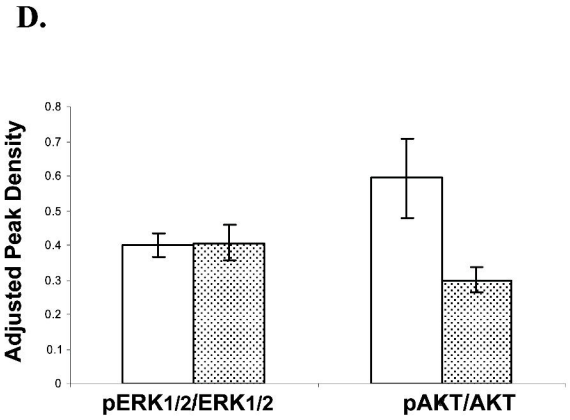

Figure 4

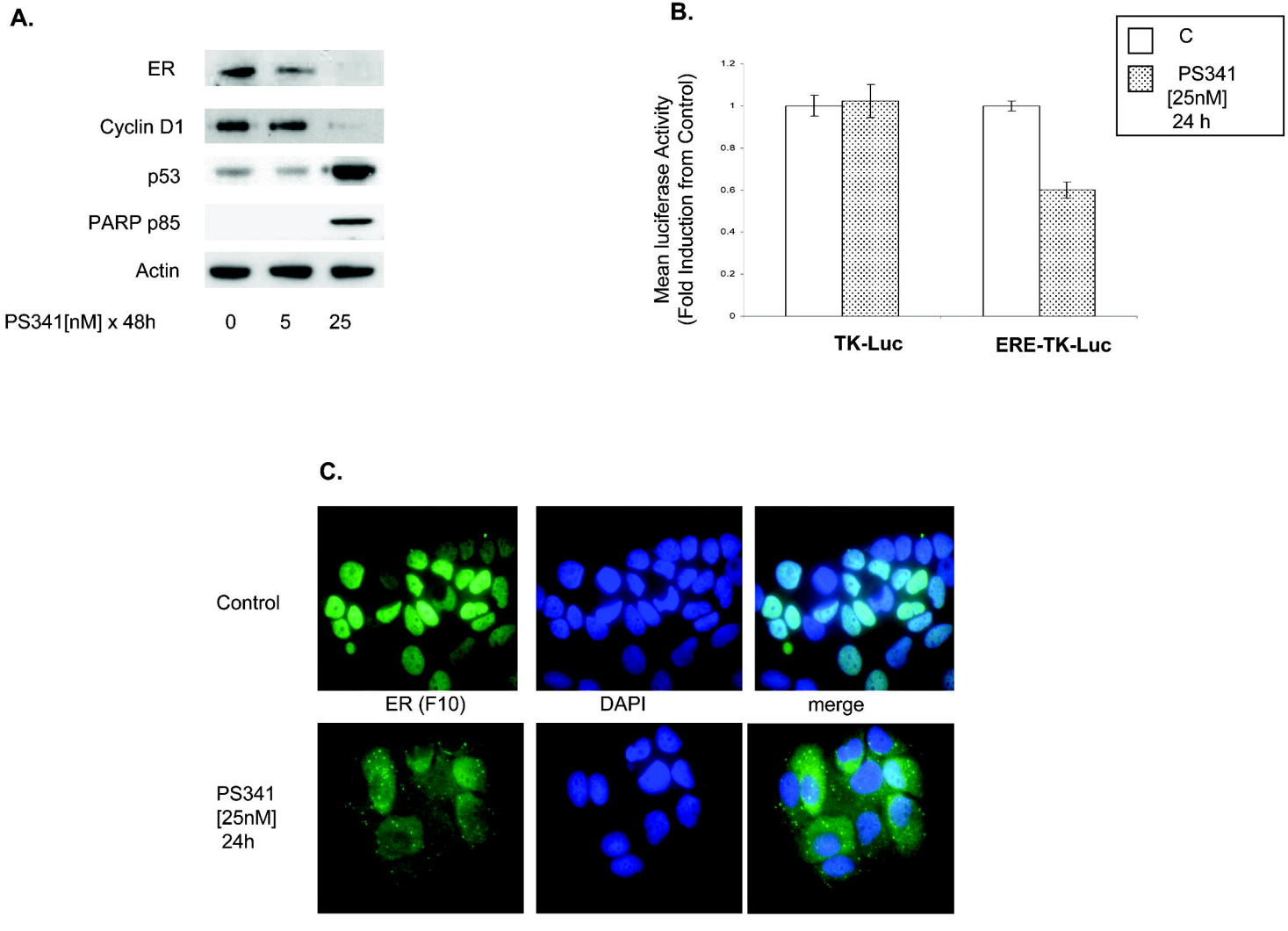

Figure 5